GT2013-94614

ASSESSMENT OF A DOUBLE HOLE FILM COOLING **GEOMETRY USING S-PIV AND PSP**

Lesley M. Wright, Stephen T. McClain, Charles P. Brown, and Weston V. Harmon

Department of Mechanical Engineering **Baylor University** Waco, TX 76798-7356 Lesley Wright@Baylor.edu

ABSTRACT

A novel, double hole film cooling configuration is investigated as an alternative to traditional cylindrical and fanshaped, laidback holes. This experimental investigation utilizes a Stereo-Particle Image Velocimetry (S-PIV) to quantitatively assess the ability of the proposed, double hole geometry to weaken or mitigate the counter-rotating vortices formed within the jet structure. The three-dimensional flow field measurements are combined with surface film cooling effectiveness measurements obtained using Pressure Sensitive Paint (PSP). The double hole geometry consists of two compound angle holes. The inclination of each hole is $\theta = 35^{\circ}$, and the compound angle of the holes is $\beta = \pm 45^{\circ}$ (with the holes angled toward one another). The simple angle cylindrical and shaped holes both have an inclination angle of $\theta = 35^{\circ}$. The blowing ratio is varied from M = 0.5 to 1.5 for all three film cooling geometries while the density ratio is maintained at DR = 1.0. Time averaged velocity distributions are obtained for both the mainstream and coolant flows at five streamwise planes across the fluid domain (x/d = -4, 0, 1, 5,and 10). These transverse velocity distributions are combined with the detailed film cooling effectiveness distributions on the surface to evaluate the proposed double hole configuration (compared to the traditional hole designs). The fanshaped, laidback geometry effectively reduces the strength of the kidney-shaped vortices within the structure of the jet (over the entire range of blowing ratios considered). The three-dimensional velocity field measurements indicate the secondary flows formed from the double hole geometry strengthen in the plane perpendicular to the mainstream flow. At the exit of the double hole geometry, the streamwise momentum of the jets is reduced (compared to the single, cylindrical hole), and the geometry offers improved film cooling coverage. However, moving downstream in the steamwise direction, the two jets form a single jet, and the counter-rotating vortices are comparable to those formed within the jet from a single, cylindrical hole. These strong secondary flows lift the coolant off the surface, and the film cooling coverage offered by the double hole geometry is reduced.

NOMENCLATURE	
C_{air}	Concentration of oxygen in the mainstream
C_{mix}	Concentration of oxygen in the air/coolant mixture
	above the plate
C_{N2}	Concentration of oxygen in the coolant
d	Diameter of the film hole
DR	density ratio = ρ_c / ρ_m
I	Measured intensity emission of PSP
I_{ref}	Reference intensity of PSP without mainstream flow
M	Blowing ratio (= $\rho_c U_c / \rho_m U_m$)
N	Number of samples for mean velocity calculations
$N_{\rm v}$	Number of vectors within interrogation region
P	Lateral pitch of film holes or pressure
P_{ref}	Reference pressure (atmospheric pressure)
$(P_{O2})_{air}$	Partial pressure of oxygen with air as coolant
$(P_{O2})_{mix}$	Partial pressure of oxygen with nitrogen as coolant
S_{v}	Standard deviation in velocity magnitude
t	Student's t-distribution
T_c	Coolant temperature
$T_{\mathbf{f}}$	film temperature
T_{m}	Mainstream temperature
$\overline{\mathbf{u}}$	Local mean velocity of coolant in x-direction
\mathbf{u}_{i}	Instantaneous velocity in x-direction
U_{c}	Mean coolant velocity
U_{m}	Mainstream velocity
V	Local magnitude of coolant velocity
\overline{v}	Local mean velocity of coolant in x-direction
$v_{\rm i}$	Instantaneous velocity in y-direction
V_{yz}	Two-component velocity magnitude (y and z components)
$\overline{\mathbf{w}}$	Local mean velocity of coolant in z-direction
w' _{RMS}	Local velocity fluctuation of coolant in z-direction
\mathbf{W}_{i}	Instantaneous velocity in z-direction

- x Streamwise distance along the flat plate
- y Spanwise distance along the flat plate
- z Perpendicular distance from the flat plate
- α Lateral angle for shaped film cooling holes (10°)
- β Compound angle of film cooling hole (45°)
- γ Laidback angle for shaped film cooling holes (10°)
- η Film cooling effectiveness
- $\bar{\eta}$ Laterally averaged film cooling effectiveness
- η_{CL} Film cooling effectiveness along the centerline (z = 0)
- ρ_c Coolant density
- ρ_m Mainstream density
- θ Streamwise inclination of the film hole (35°)

INTRODUCTION

Cooling technology for turbine airfoils has evolved over the last several decades. As manufacturing techniques progress, more advanced cooling schemes are incorporated into the While the specific cooling turbine blades and vanes. configuration will vary from engine – to – engine, today's high pressure turbine stages utilize both internal and external cooling. The hollow airfoils incorporate a variety of roughness elements to enhance heat transfer from the blade wall to the high pressure coolant passing through the internal passages. This coolant air is expelled from the interior of the airfoil to the exterior through discrete film cooling holes strategically machined into the blades and vanes. Due to the geometry of the discrete holes, the coolant forms a protective film on the outer surface of the airfoil, creating an additional layer of resistance (protection) between the hot mainstream gas and the airfoil.

With film cooling being the first layer of defense against the hot mainstream gas, it is vital the film cooling and mainstream interaction is well understood. Decades of research have indicated that film cooling performance is a function of both film cooling hole geometry and coolant flow conditions (relative to the mainstream flow). Han et al. [1] has provided a comprehensive review of film cooling parameters including film hole geometry (shape, orientation angle, and spacing) and flow conditions (mainstream turbulence intensity, blowing ratio, density ratio, and momentum flux ratio).

The film cooling protection offered by traditional, round (cylindrical) film cooling holes is strongly affected by the ejection angle of the hole and the coolant – to – mainstream blowing ratio. Decreasing the injection angle of the hole allows the coolant to remain attached to the film cooled surface while minimizing interaction with the mainstream flow. Studies have also shown a blowing ratio exists in which optimum coverage is afforded by the cooling geometry. For simple angle, cylindrical holes, this optimum blowing ratio is approximately M=0.6. As the mass flux of the coolant increases above 0.6, the increased momentum of the coolant allows the coolant to penetrate the mainstream flow, and thus liftoff the surface [1, 2].

Goldstein et al. [3] experimentally considered film cooling holes with expanded exits. By increasing the cross-sectional area at the exit of these shaped holes, the momentum of the coolant exiting the hole is reduced. With the reduced coolant velocity, the coolant remains attached to the surface even at elevated blowing ratios. The enhanced performance of shaped holes was later confirmed by Gritsch et al. [4]. Recently Wright et al. [5] showed that compared to single angle, cylindrical holes, the film cooling effectiveness on a flat plate with fanshaped, laidback film cooling holes is relatively insensitive to blowing ratio (M = 0.25 - 1.5). While this finding deviates from the trends observed for cylindrical holes, it offers positive information to engine designers as adequate protection is offered by the shaped geometry over a wide-range of engine conditions.

Separate, discrete holes are generally used for airfoil cooling to maintain the structural integrity of the hardware. However, two-dimensional, continuous slots have proven to provide increased film cooling performance compared to discrete holes [6]. To replicate the effect of the continuous slot using discrete holes, researchers have introduced the concept of trenched (or cratered) holes [7 - 9]. Entrenched holes can result from the "masking" of film holes during the thermal barrier coating (TBC) coating process. The film holes are masked before the TBC is applied to the surface of the airfoil. After the TBC is applied, the mask is removed, and the film holes are recessed in a shallow trench. As the coolant exits the hole, it fills the trench, and ultimately creates the effect of slot injection. The momentum of the coolant is reduced, it spreads laterally over an increased area, and the film cooling effectiveness on the surface is enhanced.

Continuous slots are not only advantageous as they spread the coolant over a large area, but coolant exiting the slots is predominantly two-dimensional. The coolant exiting the discrete holes, is highly turbulent and three-dimensional. This three-dimensional interaction with the mainstream reduces the overall effectiveness of the coolant. As the discrete cooling jets are injected into mainstream, a pair of counter rotating vortices forms within the jet [10 - 12]. These kidney bean shaped vortices pull the coolant away from the surface while allowing the mainstream fluid to infiltrate the space near the surface. As the formation of these counter-rotating vortices is detrimental to film cooling performance, various methods have been proposed to mitigate the formation of these vortices [13 - 21]. These studies have included a variety of tabs to generate vortices that will counteract the naturally forming vortex pair [13 - 16] and anti-vortex holes that allow additional coolant to be injected into the boundary layer near the primary film cooling hole and again weaken the kidney vortices [18 - 21]. Strategically placing the anti-vortex holes can effectively mitigate the vortices formed within the jet and significantly increase the film cooling performance.

As coupled film cooling holes have proven to be a viable alternative to the traditional round or shaped holes, it is desirable to develop a geometry that utilizes a pair (or group) of cylindrical film cooling holes of approximately the same diameter. Effectively utilizing round holes will reduce the manufacturing cost associated with shaped holes. Coupling

holes with similar diameters will provide more uniform flows while minimizing the likelihood of blockage in smaller holes. To build on this concept of paired holes, the present investigation will experimentally study a novel, double hole film cooling geometry. The proposed double hole configuration will be compared to both cylindrical and shaped hole geometries. To fully characterize the performance of the double hole design, three-dimensional flow field distributions will be obtained using stereoscopic particle image velocimetry (S-PIV). These flow measurements will be coupled with surface film cooling effectiveness measurements obtained using the pressure sensitive paint (PSP) mass transfer method. The performance of the three film cooling geometries will be evaluated at blowing ratios of M = 0.5, 1.0, and 1.5 to determine the viability of the proposed geometry compared to traditional cooling configurations.

EXPERIMENTAL FACILITIES

The low speed, open loop wind tunnel used for this experimental investigation was previously used by Wright et al. [22]. **Figure 1** shows air enters the 15.24 cm X 10.16 cm test section after traveling through multiple screens and a 2:1 contraction. The mainstream velocity through the tunnel is 10 m/s, and is monitored using a pitot-static probe placed in the center of the tunnel upstream of the film cooled flat plate.

The bottom wall of the wind tunnel is removable, so inserts with various film cooling geometries can be interchanged. A plenum attaches to the flat plate to evenly distribute the cooling air among the row of film cooling holes. For the present investigation, unheated air (or nitrogen) is supplied as the coolant, so the coolant – to – mainstream density ratio is maintained at DR = 1. To study the effect of blowing ratio, the mass flow rate of the coolant is varied to match the blowing ratios of M = 0.5, 1.0, and 1.5. For all three hole shapes (single cylindrical, shaped, and double cylindrical), a single row of seven holes is investigated. Therefore, all three designs require the same amount of coolant flow for a given blowing ratio.

Figure 2 presents the details for the film cooling geometries used in this study. Both the single, cylindrical and fanshaped, laidback holes were previously used by Wright et al. [5] to consider the effects of freestream turbulence intensity and coolant – to – mainstream density ratio. The simple angle, cylindrical hole has an inclination angle of $\theta = 35^{\circ}$, and the holes are spaced four diameters apart. The fanshaped, laidback hole also has an inclination angle of 35° . As with the cylindrical hole, the metering section of the hole has a diameter of d = 0.475 cm, and the blowing ratio for this shaped hole is based on the velocity within the cylindrical region. To form the expanded outlet of the hole, the hole opens $\alpha = 10^{\circ}$ in the spanwise direction and $\gamma = 10^{\circ}$ into the plate (perpendicular to the flow). The shaped holes are also spaced four diameters apart to prevent any jet – to – jet interaction.

The double, cylindrical hole geometry consists of three pairs of double holes (and a seventh unpaired hole). The

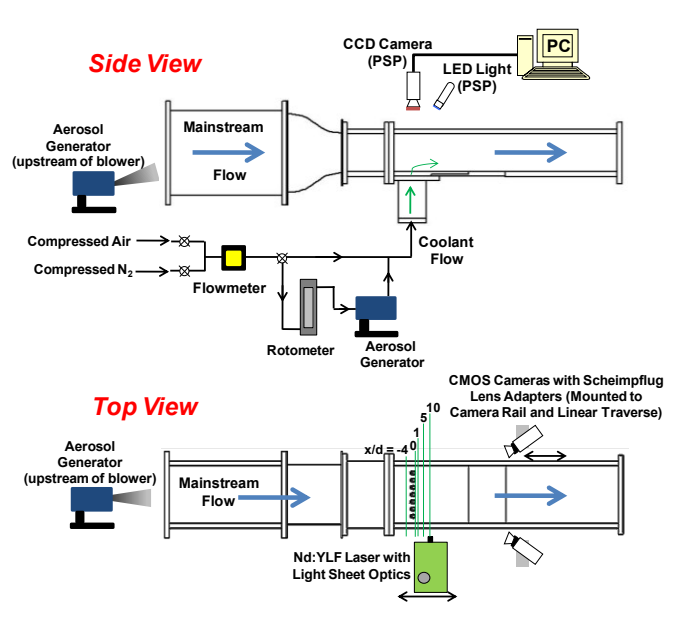


Figure 1: Overview of the Low Speed Wind Tunnel

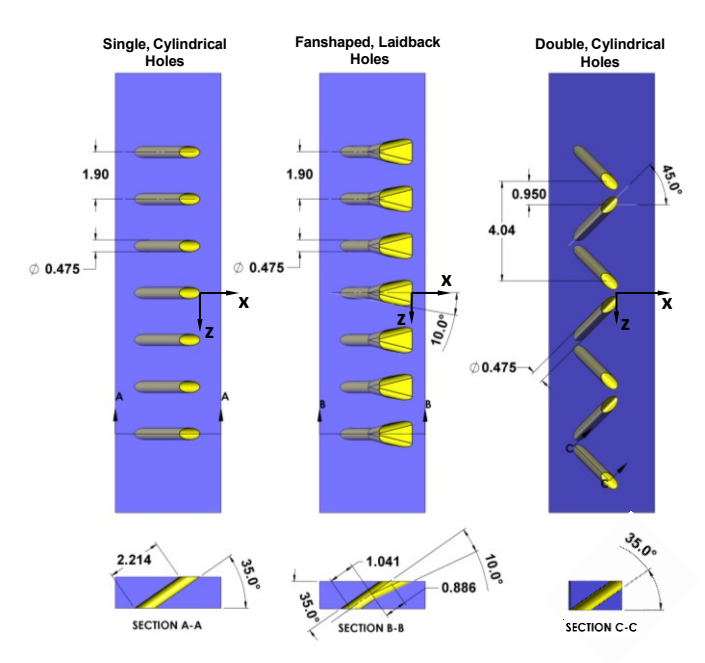


Figure 2: Details of the Film Cooling Geometries (units in [cm])

compound angle holes are also inclined 35° through the plate. The holes are also oriented at $\beta=\pm$ 45° in the spanwise direction to create the jet – to – jet interaction. The spacing of the jets was chosen to allow for mixing of the separate coolant streams to occur at the outlet of the jets (with the prescribed angles of 45° and 35°). The jet diameter is maintained for all three cooling geometries (d = 0.475 cm).

The coolant – to – mainstream interaction is investigated via the consideration of five separate measurement planes. As shown in Fig. 1, flow field measurements are taken on transverse measurements planes at x / d = -4, 0, 1, 5, and 10. The two high-speed CMOS cameras are mounted on a linear traverse, so they can be easily moved from plane – to – plane with minimal optical adjustment between planes. The laser

(with light sheet optics) is also moved to illuminate each discrete plane.

DATA REDUCTION

Stereoscopic – Particle Image Velocimetry

A stereoscopic particle image velocimetry (S-PIV) technique was used to obtain time averaged, three-dimensional velocity distributions along the film cooled flat plate. The S-PIV system used in this investigation was assembled by LaVision, Inc. and the data processing was completed using the DaVis 8.1.1 software. For the 3D velocity measurements, two high speed CMOS cameras from Vision Research (V211) were installed downstream of the film cooling holes, with one camera on each side of the tunnel (Fig. 1). At the full resolution of 1280 x 800 pixels, the cameras are capable of recording 2190 frames per second. In the current investigation, the full resolution was used, and the cameras recorded 1000 images pairs at 2000 frames per second. Both cameras were equipped with a 50mm focal length lens. In order to properly align the cameras on the measurement plane (as the cameras are not perpendicular to the measurement plane), each lens was attached to a Scheimpflug adapter which then attached to the camera. The Scheimpflug adapter is required so the camera can focus on the measurement plane which is not parallel to the camera. By viewing the measurement plane at an angle, it is possible to the capture the "out-of-plane" velocity component, and thus, simultaneously measure all three velocity components. An Nd:YLF dual cavity diode laser from Photonics Industries was used to illuminate the measurement plane. repetition rate (up to 10 kHz per head) laser produces a 532 nm laser beam, and a cylindrical lens with a focal length of f = -20mm spreads the beam into a laser light sheet. Two LaVision aerosol seeders were used to create oil droplets that were dispersed in both the mainstream and coolant flows. The seeders are capable of producing 1 µm DEHS oil particles. The flow rate through both seeders was adjusted for each flow condition to ensure the flows were properly seeded for each test.

To accurately capture the secondary flows developed within the jet, the cameras and laser were oriented such that the dominant velocity component (the streamwise velocity in the xdirection) travels through the laser sheet. To properly capture this velocity, all tests (over the range of blowing ratios) were run with a laser separation time of 25 µs. Prior to running the seeded flow experiments, a spatial calibration was completed to accurately account for the varied viewing angles from the two cameras. With the spatial calibration, depth of field was also taken into account for the ultimate calculation of the threedimensional velocity field. Due to the surface attachment of the coolant exiting the fanshaped, laidback holes, background subtraction was performed to reduce the laser reflection in the near wall region. With the coolant flow remaining attached to the surface, near wall seeding enhanced the reflection of the laser from the wall; therefore, it was necessary to remove this reflection before completing the image analysis. Prior to the

shaped hole tests, a set of reference images was recorded; the reference images were acquired by seeding only the coolant flow. These 1000 reference images were averaged (on a per pixel basis), and this average intensity at each pixel was subtracted from the corresponding pixel for each of the 1000 test images. No background subtraction was required for the single, cylindrical and double, cylindrical geometries.

After the image pairs were recorded, they were processed using the DaVis software. A multi-pass, stereo-cross correlation was used to analyze the movement of the seed particles. A total of five passes were used to calculate the velocity field, and in each pass a 50% overlap of the interrogation regions was utilized. With each pass the size of the interrogation region was reduced: 64 x 64 pixels, 32 x 32 pixels, 16 x 16 pixels, 12 x 12 pixels, 8 x 8 pixels. After calculation of the velocity vectors, the signal – to – noise ratio of the vectors were checked. Vectors having a signal-to-noise threshold ratio less than 1.1 were removed.

The mean velocity components and velocity magnitudes were calculated according to the following equations.

(x-direction)
$$\overline{u} = \frac{1}{N} \sum_{i=1}^{N} u_i$$
 (1)

(y-direction)
$$\bar{v} = \frac{1}{N} \sum_{i=1}^{N} v_i$$
 (2)

(z-direction)
$$\overline{w} = \frac{1}{N} \sum_{i=1}^{N} w_i$$
 (3)

(velocity magnitude)
$$V = \sqrt{\overline{u}^2 + \overline{v}^2 + \overline{w}^2}$$
 (4)

Because of the high accuracy laser timing and because of the spatial calibration schemes used by the LaVision system [23], the systematic uncertainties (biases) of the PIV measurements are expected to be small compared to the random uncertainties. The random uncertainties are dominated by the variations in the velocity measurements caused by the actual The random uncertainty turbulent velocity fluctuations. associated with the turbulent velocity fluctuations may be estimated using $tS_{\nu}/\sqrt{N_{\nu}}$, where t is the Student's-t distribution value, S_V is the standard deviation in the velocity magnitude (equal to the RMS fluctuating velocity component), and N_v is the number of vectors at the interrogation area. The areas of the experimental measurement with the highest turbulent fluctuating velocity components were inside the jet-freestream mixing In these regions, the maximum RMS fluctuating components were on the order of 1 m/s for the highest blowing ratio studied. Using this value as the worst case scenario, the maximum random uncertainties in the time averaged results (based on 1000 images) is 0.06 m/s.

Pressure Sensitive Paint for Film Effectiveness Measurements

Rather than employing a conventional heat transfer experiment, the film cooling effectiveness was measured using

pressure sensitive paint (PSP) [24 – 26] in a separate set of test from the S-PIV tests. Wright et al. [25] has detailed the theory and application of PSP for film cooling effectiveness measurements, so only an overview is presented here. The test plate was sprayed with the Uni-FIB PSP (UF470-750) supplied by Innovative Scientific Solutions, Inc. (ISSI). The PSP was excited using a 400 nm LED light, and a 1600 x 1200 resolution CCD (charge-couple device) camera with a 570 nm filter recorded the intensity emitted by the PSP.

The PSP was calibrated by placing a sample piece (coated with PSP) into a vacuum chamber. The pressure within the chamber is controlled, and at various pressures, the intensity emitted by the PSP was recorded. A relationship between the measured pressure and intensity of the light emitted by the paint was developed. This calibration data could then be utilized to determine the pressure on the film cooled plate from the measured light intensity.

The film cooling effectiveness was measured based on a mass transfer technique. Two similar tests were required to calculate the film cooling effectiveness: one with air as the coolant and one with nitrogen as the coolant. The film cooling effectiveness can be calculated based on the concentration of oxygen, and that is related to the partial pressure of oxygen. Therefore, the film cooling effectiveness can be calculated using Equation 5.

$$\eta = \frac{T_f - T_m}{T_c - T_m} = \frac{C_{mix} - C_{air}}{C_{N_2} - C_{air}} = \frac{C_{air} - C_{mix}}{C_{air}} = \frac{\left(P_{O_2}\right)_{air} - \left(P_{O_2}\right)_{N_2}}{\left(P_{O_2}\right)_{air}}$$
(5)

This mass transfer analogy has been compared directly to more established steady state [25] and transient heat transfer techniques [27]. The PSP technique has been directly validated against steady state infrared thermography (IR) and temperature sensitive paint (TSP) measurements on a film cooled flat plate. The effectiveness measurements obtained on the flat plate from these three techniques were within 13% of one another at M = 0.6, and at M = 1.2, the three techniques yielded results within 3%. The PSP technique has been utilized by researchers at Baylor University [5, 28]. In these investigations, film cooling effectiveness measurements obtained on flat plates under a variety of flow conditions (blowing ratios, density ratios, and free stream turbulence intensities) have been directly compared to published data. The PSP results compared favorably to published data; moving six diameters downstream of the holes, the PSP data was generally within 5% of published data. Furthermore, Wright et al. [22] successfully coupled 2D PIV measurements with surface film cooling effectiveness distributions from PSP. Coupling the surface and flow field measurements further validated the PSP technique, as the flow phenomena captured by the PIV was directly related to the attachement of the film coolant on the surface. As the PSP technique has proven to be a valid method for obtaining detailed film cooling effectiveness distributions, it will be utilized in this current investigation.

Experimental uncertainty was considered using the method presented by Kline and McClintock [29]. The uncertainty of the film effectiveness measurements varies depending on the intensity level measured by the CCD camera. The experimental uncertainty is less than 8% for film effectiveness measurements greater than 0.65. However, as the effectiveness begins to approach zero (where the measured light intensities are relatively low), the uncertainty rises. For a film cooling effectiveness of 0.08, the uncertainty is approximately 15%, and continues to rise as the effectiveness approaches zero. All experimental results were repeated multiple times to confirm the repeatability of the data. The data proved to be repeatable within the experimental uncertainty for the entire range of film effectiveness that was measured.

RESULTS AND DISCUSSION

To assess the viability of the present double hole geometry, the flow structure and surface film cooling effectiveness of the proposed geometry are compared to those of the simple, cylindrical and fanshaped, laidback geometries. Before evaluating the performance of the film cooling configurations, the flow conditions upstream of the film cooling holes is established. With knowledge of the mainstream flow conditions, the flow structure of the three film cooling designs can be compared. Finally, the stereo-PIV measurements are coupled with surface film cooling effectiveness measurements to consider both the thermal and fluid flow fields.

Mainstream Flow Conditions

With the mainstream seeded independently of the cooling flow, it is possible to characterize the freestream flow upstream of the film cooling holes. Figure 3 shows the freestream velocity distribution obtained four diameters upstream of the film cooling holes. The normalized velocity magnitude takes into account all three velocity components obtained from the stereoscopic-PIV measurements (although for this upstream plane, the velocity magnitude is dominated by the streamwise [x] component). At approximately three diameters above the test surface, the local velocity converges to the measured freestream velocity (V/ $U_m \approx 1$). The velocity measurements indicate the flow is uniform across the span of the wind tunnel. The measured, streamwise velocity profile is compared to that approximated by the 1/7th power law profile. Within the power law profile, the boundary layer thickness has been approximated based on a freestream Reynolds number 112,600 (with the characteristic length measured from the exit of the upstream contraction to the measurement plane). The velocity measurements indicate the boundary layer approaching the film cooling holes is thicker than that predicted by the 1/7th profile. The figure also shows the turbulent fluctuations are suppressed near the wall, and near the center of the tunnel, the turbulent fluctuations are approximately 8%. This is elevated above the values reported from previous investigations using this tunnel due to the installation of a new blower and the removal of one of the screens in the inlet section of the tunnel.

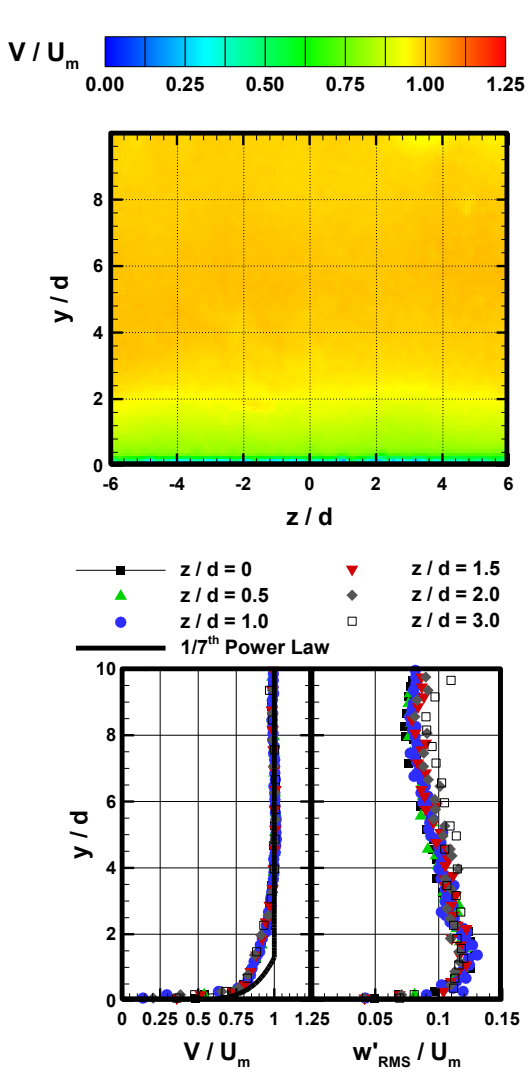


Figure 3: Mainstream Velocity Distribution Upstream of the Film Cooling Holes (x/d = -4)

Flow Structure of Simple Angle, Cylindrical Holes

Before presenting the flow structure of the shaped and double hole geometries, it is necessary to consider the structure of the baseline, cylindrical hole with the simple injection angle of 35° . **Figure 4** presents the velocity distributions measured at each downstream plane at the highest blowing ratio of M=1.5. The flowfield above only the centermost hole is shown in the figure, and the distributions are divided to isolate the non-streamwise velocity components. The three-component, normalized velocity is shown on the left side of each figure, and normalized, two-component velocity is shown on the right. The two component velocity magnitude is defined in Equation 6.

$$V_{yz} = \sqrt{\overline{v}^2 + \overline{w}^2} \tag{6}$$

As the streamwise velocity component (x-direction) dominates the velocity magnitude, removing this component highlights the strong secondary flows formed within the cooling jet.

As the coolant immediately exits the cylindrical hole (x/d = 0), the counter-rotating vortex pair is observed. Near the surface, the central core of the jet is being lifted vertically off the surface. Moving one diameter downstream of the hole exit (x/d = 1), this high blowing ratio cooling jet is lifting off the

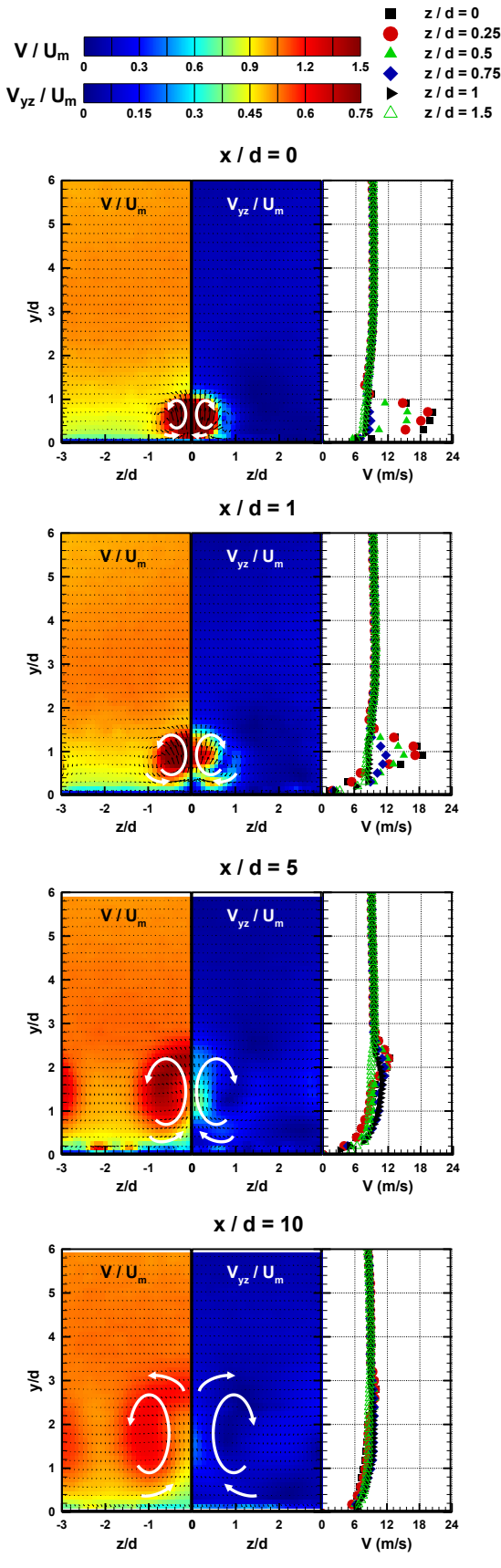


Figure 4: Velocity Distributions Downstream of the Single, Cylindrical Holes (M = 1.5)

surface. As the jet is detaching from the surface, the mainstream air is being entrained into the jet, and the jet is spreading over an increased area. It is interesting to observe the strong transverse velocity occurring along the lower peripheral

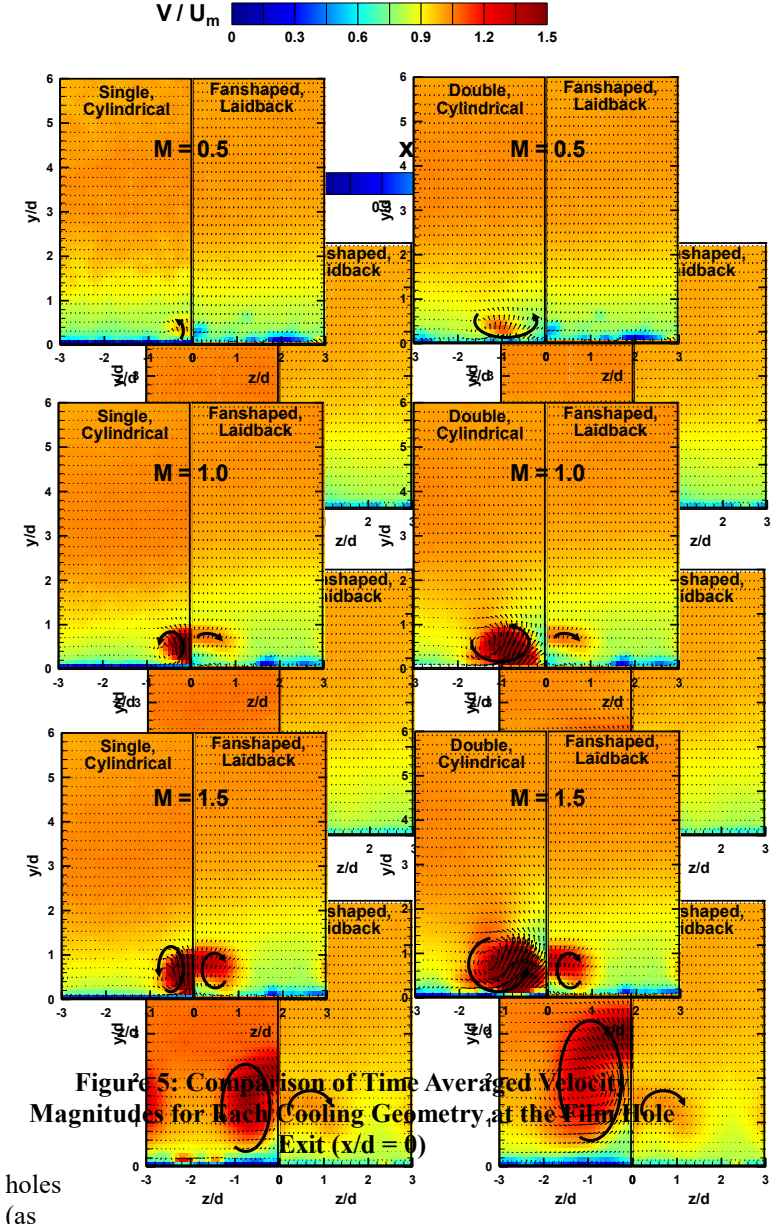
of the jet (z/d=0.5). This transverse velocity distribution clearly indicates the mainstream fluid is being pulled under the cooling jet, and thus in contact with the film cooled surface. Continuing downstream (x/d=5 and 10), the y and z velocity components weaken as the coolant becomes sufficiently mixed with the mainstream fluid. However, the presence of the counter-rotating vortices remains apparent.

Effect of Hole Shape on Cooling Jet Structure

The time averaged velocity magnitudes are compared for each hole geometry in Figures 5 and 6. The flow fields at x/d = 0 are compared for each blowing ratio in **Figure 5**. The figures on the left directly compare the flow fields from the traditional cylindrical holes to those from the current, fanshaped, laidback hole. The most notable difference between the two hole shapes is the reduced velocity from the shaped holes. Both the three-component velocity magnitude and the secondary velocity in the y-direction are lower for the shaped holes compared to the single, cylindrical holes. With the cylindrical hole, the counter-rotating vortex pair clearly lifts the coolant from the surface, and the mainstream is entrained below the coolant. A counter-rotating vortex forms within the jet from the shaped hole; however, the strength of this vortex is significantly weaker compared to the cylindrical jet. Moreover, the expanded exit area of the shaped hole allows the coolant to spread laterally over a larger area (further reducing the coolant velocity and providing protection over an increased spanwise area). With the reduced velocity, the coolant more readily stays attached to the flat plate. Near the surface, the velocity from the shaped holes is clearly less that from the cylindrical hole. Furthermore, with the reduced strength of the counter-rotating vortex pair, the entrainment of the mainstream fluid under the jet is reduced. Although Fig. 5 indicates the core of the coolant has lifted from the surface, the reduced velocity near the surface is expected due to the no-slip boundary at the wall. While both the cylindrical and shaped holes exhibit similar secondary flow patterns, the most significant benefit of the fanshaped, laidback geometry is the reduced momentum of the coolant exiting the hole.

The composite distributions on the right side of Fig. 5 allow for the direct comparison of the proposed double hole geometry to the current shaped hole. The current double hole geometry was developed with the intention of creating a destructive interaction of the counter-rotating vortices formed within each separate jet. However, from the velocity distributions shown in Fig. 5, rather than mitigating the vortex pairs, the combined secondary flows strengthen the secondary flows within the coolant. When the two separate jets collide and form a single jet, this combined jet contains significantly more coolant than the cylindrical or shaped holes.

At the lowest blowing ratio of M = 0.5, the central core of the coolant from the double hole geometry is offset from the centerline approximately one jet diameter (z/d = -1). With the centerline being located between the two holes, this indicates a clear separation of the two jets as they exit their respective



x/d=0

the
offset
core

Figure 6: Comparison of Time Averaged Velocity
Magnitudes Downstream of Each Film Cooling
Geometry (x/d = 5)

ents the core of a single jet). However, as the blowing ratio increases, the jet spreads laterally, and the velocity within the jet increases. As the jets spread they interact with one another, and the counter-rotating vortices strengthen. The size and strength of the vortex is significantly greater for the double hole than the single hole geometry.

Moving further downstream, the structure of the coolant jet changes for all three hole configurations. **Figure 6** shows the time averaged velocity distributions at x/d = 5. For all three hole shapes at M = 0.5, the mainstream flow is only marginally disturbed by the coolant at this downstream location. With the relatively low blowing ratio of the coolant, both the streamwise and secondary flow structures are weak compared to the mainstream. At this downstream location the core of the coolant has shifted toward the center of the double hole geometry (between the two cylindrical holes). This indicates

repres

the once separate jets have formed a single jet as it continues downstream. Similar to the single, cylindrical hole, the counterrotating vortex is lifting the coolant from the surface.

As the two jets collide to form a large, single jet, the counter-rotating vortices within the coolant dominate the film cooling performance. Figure 6 shows the physical size of the kidney vortex is approximately four times as large as the vortex in the shaped jet (twice as large in the y-direction and twice a large in the z-direction). While the disparity is not as great comparing the double hole to the single hole, the coolant is lifting further off the surface with the double hole. This large area of circulation enhances mixing with the mainstream, and this increased mixing is detrimental to the film cooling performance. The coolant - to - mainstream mixing increases the local turbulence while allowing the mainstream fluid to become entrained beneath the jet (in direct contact with the surface). At this downstream location, the double hole is also outperformed by the single hole geometry. With the increased momentum of the combined jets, the upwash of the coolant is more significant than measured within the single hole. The increased velocity in the y-direction will lead to reduced film cooling effectiveness on the surface.

The coolant flows associated with the cylindrical and shaped holes are consistent with those shown in Fig. 5. The vortex pair within the cylindrical jet has spread over a larger area (with reduced velocity to compensate for the increased area). As with the near-hole plane, the bulk of the coolant is lifting off the surface. Based on this secondary flow pattern, it

is believed the shaped holes will provide adequate protection moving downstream.

At the highest blowing ratio of M=1.5, the merging of the separate cooling streams is clearly show in **Figure 7**. At the downstream edge of the film cooling holes (x/d=0), two separate jets are observed. However, these relatively high momentum jets form a single jet a less than one diameter downstream. With the increased momentum within this newly formed jet, the coolant is clearly separating from the surface. At x/d=1, the maximum coolant velocity is observed 1.4 diameters above the flat plate (y/d=1.4). For the single, cylindrical hole, the core of the coolant had lifted to approximately y/d=1.0. The increased liftoff associated with the double hole geometry continues as the coolant moves downstream. Furthermore, as the coolant lifts off the surface, the counter-rotating vortices pull the mainstream fluid to the plate.

Effect of Jet Structure on Surface Film Cooling Effectiveness

With knowledge of the mainstream - to - coolant interaction on the flat plate, it is possible to see the direct impact of the coolant structure on the surface film cooling effectiveness. Figures 8-10 couple the three-component velocity magnitude distributions at each measurement plane downstream of the film cooling holes with the detailed distribution of the surface film cooling effectiveness. The

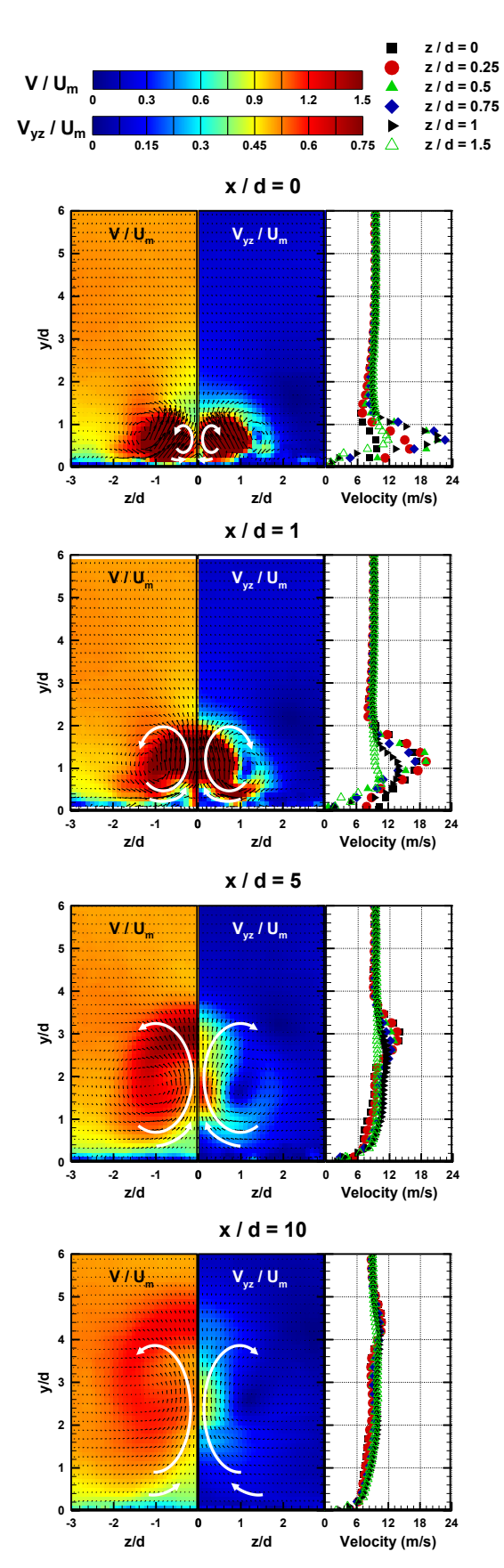


Figure 7: Velocity Distributions Downstream of the Double, Cylindrical Holes (M = 1.5)

velocity distribution at x/d = 0 is plotted with only the contour

lines to improve the visual access to x/d=1 and the effectiveness distribution.

Figure 8 shows the combined velocity and effectiveness distributions for the baseline, cylindrical hole geometry. The lowest blowing ratio of M=0.5 provides the best film cooling effectiveness as the cooling jet remains attached to the surface, and there is minimal interaction between the coolant and the mainstream. As the blowing ratio increases, the counterrotating vortices become more apparent, and the jet begins to lift off the surface. Although the surface effectiveness decreases as the blowing ratio increases, a narrow band of coolant is measured downstream of the hole (near the centerline). This slightly elevated effectiveness corresponds to the relatively low

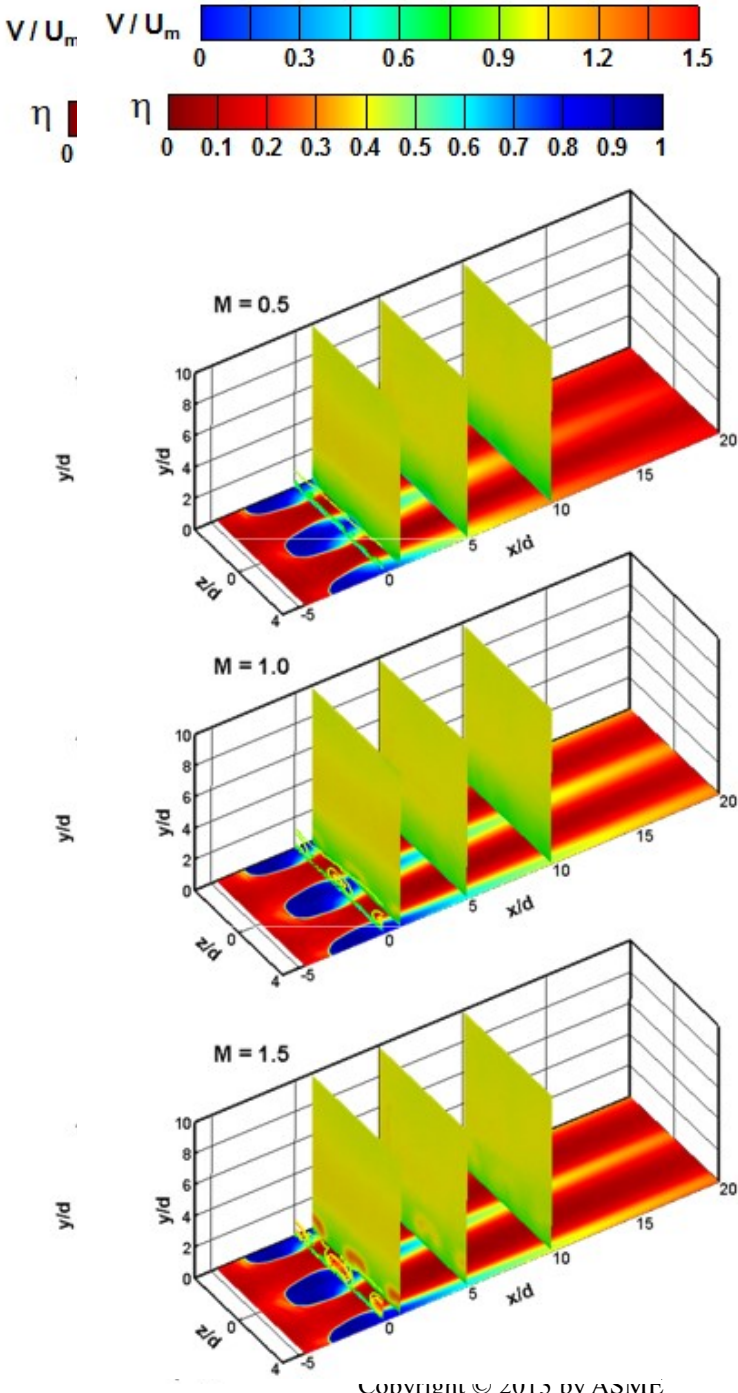


Figure 8: Congression Velocitos ffielde herit & Fii filden hilmurface Cooling Efficati Cookin Disfribitions sodishei Sirigles, for the Cylifian istan plot Laidback Hole

are relatively weak (with no lift off). It would appear the double hole geometry allows the jet to initially lift off the surface before it reattaches to the plate at x/d=3 (where a maximum effectiveness is measured). However, at this lowest blowing ratio, the jets remain separated from one another for several jet diameters downstream of the holes. When the coolant flows merge, this maximum film cooling effectiveness occurs. As interaction with the mainstream increases downstream of the holes, the film cooling effectiveness decreases. At this lowest blowing ratio, all three hole designs

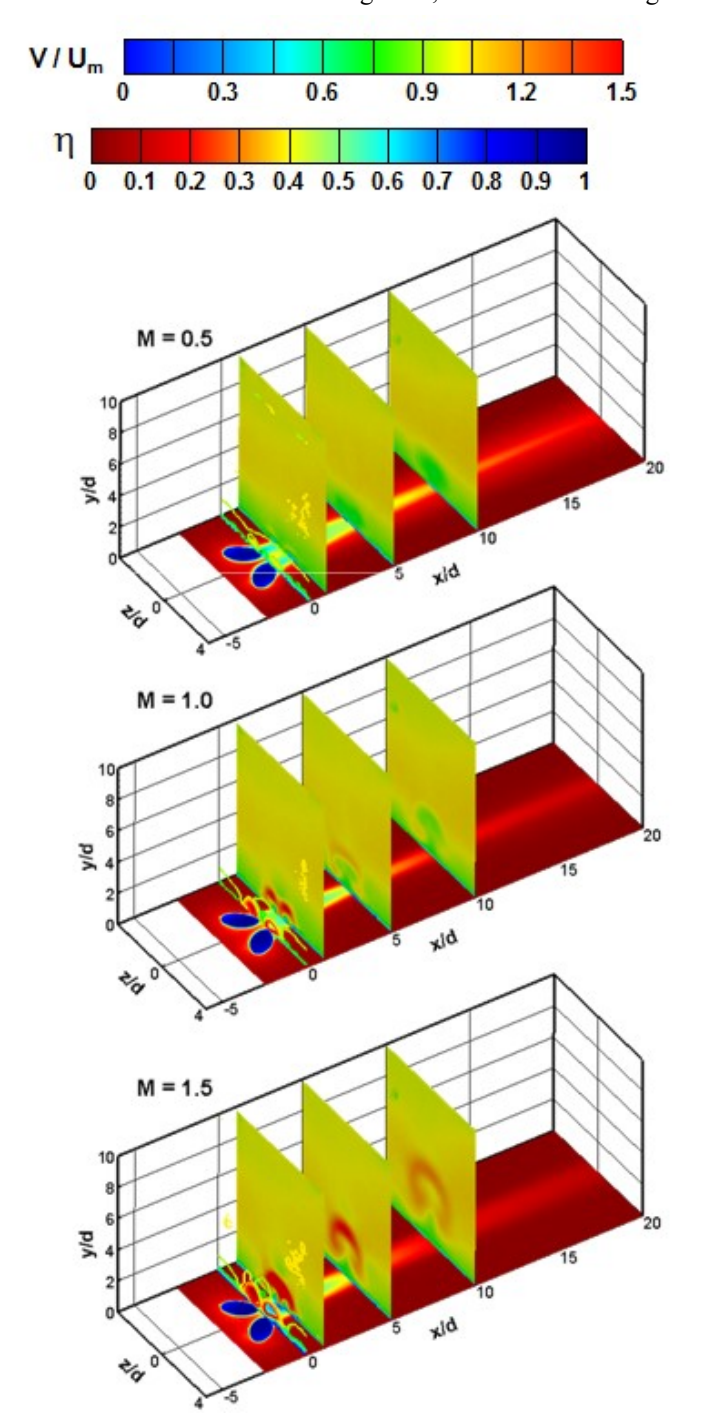


Figure 10: Composite Velocity Field and Surface Film Cooling Effectiveness Distributions for the Double, Cylindrical Hole

offer comparable levels of protection beyond x/d = 10.

At the higher blowing ratios of M = 1.0 and 1.5, the double hole design provides a film cooling effectiveness that is comparable to the shaped hole in the near hole region (x/d < 5). However, moving downstream, the effectiveness trends are more comparable to the traditional, cylindrical hole. As the separate jets initially exit the holes, the reduced streamwise momentum of the separate jets leads to an increase in the film cooling effectiveness. However, as the separate coolant streams

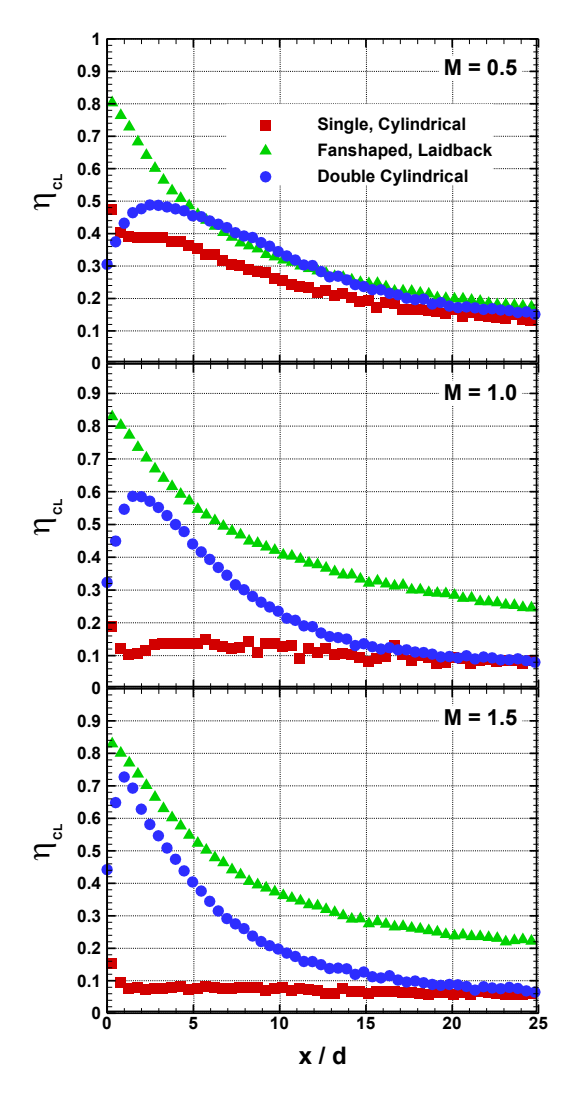


Figure 11: Centerline (z/d = 0) Film Cooling Effectiveness Comparisons

merge into a single stream, the secondary flows gain strength, mixing with the mainstream is enhanced, and as a result, the mainstream is transported to the surface. With the mainstream infiltrating the coolant flow, the film cooling effectiveness on the surface decreases.

The superiority of the fanshaped, laidback hole is shown with the laterally averaged film cooling effectiveness distributions. The lateral average distributions shown in **Figure**

12 were obtained by averaging the film cooling effectiveness over the span $-4 \le z/d \le 4$. For the traditional cylindrical and shaped holes, this distance represents two geometrical periods. For the double hole geometry, one full period is 8.5 diameters wide, so this spanwise distance is less than the full period. This spanwise distance was chosen for the averaging as the coolant mass flow is equal for all three geometries over this area (coolant protection is offered from two film cooling holes for

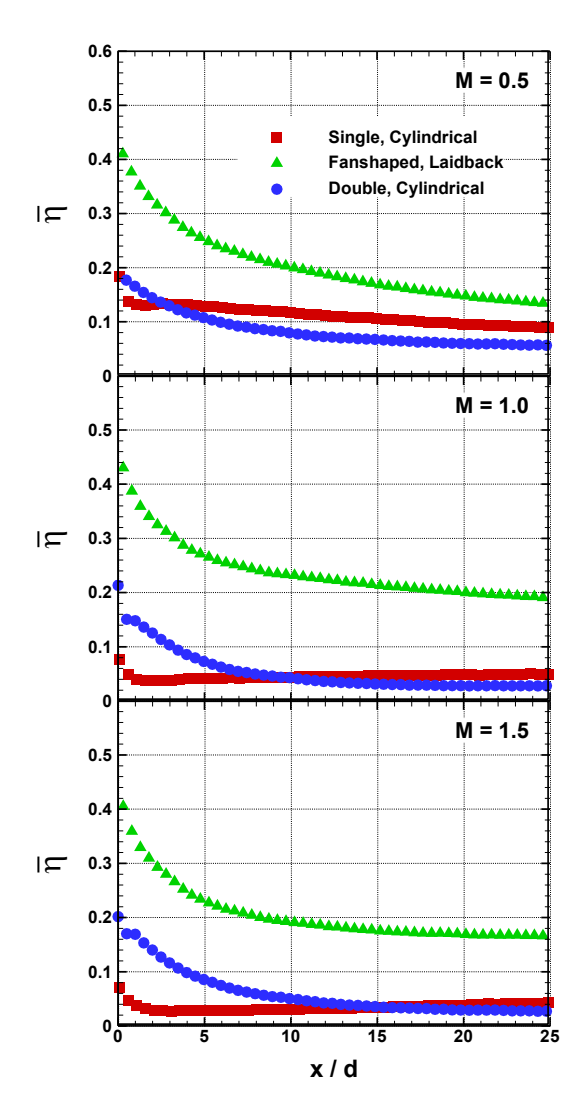


Figure 12: Laterally Averaged ($-4 \le z/d \le 4$) Film Cooling Effectiveness Comparisons

each geometry). Based on the laterally averaged film cooling effectiveness, the double hole geometry generally provides the least projection of the three designs. While it provides better protection downstream of the holes (compared to the single cylindrical hole), the spanwise spread of the coolant is limited, and a significant portion of the surface remains unprotected. Considering both the centerline and laterally averaged distributions, the surface is best protected downstream of the shaped film cooling holes.

CONCLUSIONS

An experimental study has been completed to characterize the secondary flow behavior of a film cooling geometry consisting of a pair of compound angle, cylindrical holes. This double hole geometry was compared to a traditional, single cylindrical hole geometry and a fanshaped, laidback geometry. While the proposed double hole geometry does not outperform the shaped design (based on the surface film cooling effectiveness), the performance of the double hole design is comparable to that of the shaped hole in the region immediately downstream of the hole (x/d < 5). The S-PIV measurements indicate when the jets remain separated from one another, they have reduced momentum and offer improved coverage, similar to the fanshaped, laidback geometry. However, once the two jets merge into a single jet, the single coolant stream follows the trends of the single, cylindrical hole. With the combined coolant flow rates, additional mixing of the coolant with the mainstream takes place, and the mainstream gas is transported to the surface while the coolant detaches from the surface.

the S-PIV technique Combining characterization with the PSP technique for detailed surface temperature (film effectiveness) diagnostics has led to valuable insight into the jet - to - mainstream interactions. Because the proposed geometry, which double the coolant flow rate at a given location, affords less surface protection than more traditional film cooling geometries, it is not a viable alternative to the shaped film cooling hole. Using this knowledge, a more viable double-hole geometry can be developed and tested against the more traditional cooling configurations. necessary to investigate the effect of the geometry (angle and spacing) of the paired film cooling holes with the coolant – to – mainstream flow conditions (blowing and density ratios). As the coolant jets from the separate holes interact, the attachment or separation of the coolant from the surface will be a function of the blowing ratio. Therefore, additional work is needed to realize the full potential of double hole film cooling geometries.

ACKNOWLEDGEMENTS

This work has been sponsored by the National Science Foundation under award number CBET-1126371. The authors would like to thank Dr. Truell Hyde, Vice-Provost of Research at Baylor University, and Dr. William Jordan, Mechanical Engineering Department Chair, for their support of this project.

REFERENCES

- [1] Han, J.C., Dutta, S., and Ekkad, S., 2000, *Gas Turbine Heat Transfer and Cooling Technology*, Taylor and Francis, New York, 646 pages.
- [2] Bogard, D.G. and Thole, K.A., 2006, "Gas Turbine Film Cooling," *AIAA J. Propulsion and Power*, Vol. 22, pp. 249-270.
- [3] Goldstein R.J., Eckert E.R.G., and Burgrraff, F., Effects of Hole Geometry and Density on Three-Dimensional Film

- Cooling, *International J. Heat and Mass Transfer*, Vol. 17, pp 595-607, 1974.
- [4] Gritsch, M., Schulz, A., Wittig, S., 1998, "Adiabatic Wall Effectiveness Measurements of Film-Cooling Holes with Expanded Exits," ASME J. Turbomachinery, Vol. 120, pp 549-556.
- [5] Wright, L.M., McClain, S.T., and Clemenson, M.D., 2011, "Effect of Density Ratio on Flat Plate Film Cooling with Shaped Holes using PSP," ASME J. Turbomachinery, Vol. 133, No. 4, Article 041011 (11 pages).
- [6] Papell, S.S., 1960, "Effect of Gaseous Cooling of Coolant Injection Through Angled Slots and Normal Holes," NASA Technical Note. D299.
- [7] Bunker R.S., 2002, "Film Cooling Effectiveness Due to Discrete Holes within a Transverse Surface Slot", ASME Paper No. GT-2002-30178.
- [8] Lu, Y., Nasir, H., Ekkad, S.V, 2005, "Film Cooling from a Row of Holes Embedded in Transverse Slots," ASME Paper No. GT2005-68598.
- [9] Lu, Y., Ekkad, S.V, 2006, "Film Cooling Predictions for Cratered Cylindrical Inclined Holes," ASME Paper No. IMECE2006-14406.
- [10] Margason, R.J., 1993, "Fifty Years of Jet in Cross Flow Research," AGARD, Computation and Experimental Assessment of Jets in Cross Flow.
- [11] Kelso, R.M., Lim, T.T., Perry, A. E., 1996, "An Experimental Study of Round Jets in Cross-Flow," *J. Fluid Mechanics*, Vol. 306, pp 111-144.
- [12] Haven, B.A., Yamagata, D.K., Kurosaka, M., Yamawaki, S. and Maya, T., 1997, "Anti-Kidney Vortices in Shaped Holes and Their Influence on Film Cooling Effectiveness," ASME Paper 97-GT-45.
- [13] Hyams, D. G, McGovern, K.T., and Leylek, J.H., 1996, "Effects of Geometry on Slot-Jet Film Cooling Performance," ASME paper 96-GT-187.
- [14] Haven, B.A., Kurosaka, M., 1996, "Improved Jet Coverage through Vortex Cancellation," *AIAA Journal*, Vol.34, No. 11, pp 2443-2444.
- [15] Zaman, K.B.M.Q., Foss, J.K., 1997, "The Effects of Vortex Generators on a Jet in Cross-Flow," *Physics of Fluids*, Vol.9, No. 1 pp 106-114.
- [16] Zaman, K.B.M.Q., 1998, "Reduction of Jet Penetration in a Cross-Flow by Using Tabs," AIAA Paper No. 98-3276.
- [17] Shih, T. I-P., Lin, Y.L., Chuy, M.K. and Gogineni, S., 1999, "Computations of Film Cooling from Holes with Struts," ASME Paper 99-GT-282.
- [18] Heidmann, J.D., Ekkad, S.V, 2007, "A Novel Anti-Vortex Turbine Film Cooling Hole Concept," ASME Paper No. GT2007-27528.
- [19] Dhungel. A., Lu, Y. Phillips, W., Ekkad, S.V, Heidmann, J.D., 2007, "Film Cooling from a Row of Holes Supplemented with Row of Anti Vortex Holes," ASME Paper No. GT2007-27419.
- [20] Schulz, S., Maier, S., and Bons, J.P., 2012, "an Experimental Investigation of an Anti-Vortex film cooling

- geometry Under Low and High Turbulence Conditions," ASME Paper No. GT2012-69237.
- [21] LeBlanc, C., Narzary, D., Ekkad, S., and Alvin, M.A., 2012, "Performance of Tripod Antivortex Injection Holes on Vane Film Cooling," ASME Paper No. HT2012-58135.
- [22] Wright, L.M., McClain, S.T., and Clemenson, M.D., 2011, "Effect of Freestream Turbulence on Film Cooling Jet Structure and Surface Effectiveness using PIV and PSP," ASME J. Turbomachinery, Vol. 133, No. 4, Article 041023 (12 pages).
- [23] FlowMaster Product Manual, 2011, LaVision GmbH, Germany, 176 pages.
- [24] Zhang, L.J. and Jaiswal, R.S., 2001, "Turbine Nozzle Endwall Film Cooling Study Using Pressure-Sensitive Paint," *ASME J. Turbomachinery*, Vol. 123, pp. 730-735.
- [25] Wright, L.M., Gao, Z., Varvel, T.A., and Han, J.C., 2005, "Assessment of Steady State PSP, TSP, and IR Measurement Techniques for Flat Plate Film Cooling," ASME Paper No. HT2005-72363.
- [26] Han, J.C. and Rallabandi, A.P., 2010, "Turbine Blade Film Cooling Using PSP Technique," Frontiers of Heat and Mass Transfer, Vol. 1, Article 013001 (21 pages).
- [27] Gao, Z., Wright, L.M., and Han, J.C., 2005, "Assessment of Steady State PSP and Transient IR Measurement Techniques for Leading Edge Film Cooling," ASME Paper No. IMECE2005-80146, 2005 ASME IMECE, Orlando, Florida.
- [28] Wright, L.M. and Martin, E.L., 2011, "Film Cooling Effectiveness Distributions on a Flat Plate with a Double Hole Geometry using PSP," ASME Paper No. AJTEC2011-44541, ASME/JSME 8th Thermal Engineering Joint Conference, Honolulu, Hawaii.
- [29] Kline, S.J., and McClintock, F.A., 1953, "Describing Uncertainties in a Single Sample Experiment," *Mechanical Engineering*, 75, pp. 3-8.